

Improving Link Reliability of IEEE 802.15.4g SUN with Re-Transmission Shaping

Domenico Solimini
Department of Mathematics
University of Padova
Padova, Italy
{domenico.solimini}@studenti.unipd.it

Pere Tuset-Peiró, Guillem
Boquet, Xavier Vilajosana
Wireless Networks Laboratory
Internet Interdisciplinary Institute
Universitat Oberta de Catalunya
Barcelona, Spain
{peretuset,gboquet,xvilajosana}@uoc.edu

Francisco Vázquez-Gallego
Centre Tecnològic de
Telecomunicacions de Catalunya
(CTTC/CERCA)
Castelldefels, Spain
{francisco.vazquez}@cttc.es

ABSTRACT

Packet re-transmissions are a common technique to improve link reliability in low-power wireless networks. However, since packet re-transmissions increase the end-device energy consumption and the network load, a maximum number of re-transmissions per packet is typically set, also considering the duty-cycle limitations imposed by radio-frequency regulations. Moreover, the number of re-transmissions per packet is typically set to a constant value, meaning that all packet re-transmissions are treated the same regardless of actual channel conditions (i.e., multi-path propagation or internal/external interference effects). Taking that into account, in this paper we propose and evaluate the concept of re-transmission shaping, a mechanism that manages packet re-transmissions to maximize link reliability, while minimizing energy consumption and meeting radio-frequency regulation constraints. The proposed re-transmission shaping mechanism operates by keeping track of unused packet re-transmissions and allocating additional re-transmission when the instantaneous link quality decreases due to channel impairments. To evaluate the re-transmission shaping mechanism we use trace-based simulations using a IEEE 802.15.4g SUN data-set and two widely used metrics, the PDR (Packet Delivery Ratio) and the RNP (Required Number of Packets). The obtained results show that re-transmission shaping is a useful mechanism to improve link reliability of low-power wireless communications, as it can increase PDR from 77.9% to 99.2% while sustaining a RNP of 2.35 re-transmissions per packet, when compared to using a single re-transmission per packet.

CCS CONCEPTS

• **Networks** → **Physical links; Link-layer protocols; Wireless access networks; Wireless access points, base stations and infrastructure; Network performance analysis; Network simulations.**

Permission to make digital or hard copies of all or part of this work for personal or classroom use is granted without fee provided that copies are not made or distributed for profit or commercial advantage and that copies bear this notice and the full citation on the first page. Copyrights for components of this work owned by others than ACM must be honored. Abstracting with credit is permitted. To copy otherwise, or republish, to post on servers or to redistribute to lists, requires prior specific permission and/or a fee. Request permissions from permissions@acm.org.

PE-WASUN'20, November 16–20, 2020, Alicante, Spain

© 2020 Association for Computing Machinery.

ACM ISBN 978-1-4503-8118-5/20/11...\$15.00

<https://doi.org/10.1145/3416011.3424750>

KEYWORDS

Internet of Things; IEEE 802.15.4g; Smart Utility Networks; Re-transmission Shaping

ACM Reference Format:

Domenico Solimini, Pere Tuset-Peiró, Guillem Boquet, Xavier Vilajosana, and Francisco Vázquez-Gallego. 2020. Improving Link Reliability of IEEE 802.15.4g SUN with Re-Transmission Shaping. In *17th ACM Symposium on Performance Evaluation of Wireless Ad Hoc, Sensor, & Ubiquitous Networks (PE-WASUN'20)*, November 16–20, 2020, Alicante, Spain. ACM, New York, NY, USA, 8 pages. <https://doi.org/10.1145/3416011.3424750>

1 INTRODUCTION

Achieving link reliability in low-power wireless networks has been a quest for the past decades. Various authors have proposed different strategies at the physical, data-link and network layers to cope with the intrinsic problems of the wireless channel (i.e., multi-path propagation and internal/external interference effects), while keeping a low-power consumption profile that allows devices to operate using batteries for multiple years and meeting the duty-cycle limitations imposed by radio-frequency regulations.

Given the rising interest in reliability for low-power wireless communications, the IETF (Internet Engineering Task Force) has recently chartered the RAW (Reliable and Available Wireless) group [9]. The aim of RAW is to achieve deterministic performance metrics [4], such as low packet error rate, bounded consecutive packet losses and bounded latency, over wireless links to provide high reliability and availability for IP (Internet Protocol) communications. These performance metrics are known as PAREO [8] and are key to enable the convergence between OT (Operational Technologies) and IT (Information Technologies), as demanded by the Industrial Internet.

To provide high reliability for low-power wireless communications, in this article we propose re-transmission shaping, a mechanism that keeps track of unused packet re-transmissions (i.e., packets that have been successfully received without using all the possible re-transmissions), and allows to use them in the future to maintain link reliability under adverse channel conditions caused by multi-path propagation or internal/external interference effects.

To evaluate the proposed re-transmission shaping mechanism we use simulations based on a IEEE 802.15.4g [1, 2] SUN (Smart Utility Network) data-set [12], obtained through a real-world deployment of 11 devices in a large industrial scenario, using two widely used metrics: the PDR (Packet Delivery Ratio) and the RNP (Required Number of Packets). In addition to having a low implementation

complexity, the results show that the re-transmission shaping mechanism can improve PDR significantly (i.e., from 77.4% to 99.2%) while keeping the RNP within bounds (i.e., 2.35 re-transmissions per packet) compared to single re-transmission per packet.

The remainder of this article is organized as follows. Section 2 presents the previous works related to reliability of packet delivery in low-power wireless networks. Section 3 introduces the concept of re-transmission shaping and describes a mechanism to implement it. Section 4 presents the methodology that we have used to validate the proposed re-transmission shaping mechanism. Section 5 presents and discusses the performance evaluation results obtained through simulation. Finally, Section 6 concludes the paper.

2 RELATED WORK

As introduced earlier, over the past decades various authors have studied the issues of reliability in low-power wireless communications and have proposed different strategies to cope with the intrinsic problems of the wireless channel (i.e., multi-path propagation and internal/external interference effects), while keeping a low-power profile that allows devices to operate using batteries for multiple years. In this section we briefly present various of these techniques that are implemented either at the physical, data-link or network layers, respectively.

Regarding the physical layer, in [5] the authors proposed to exploit constructive interference as a means to increase link reliability of time-synchronized IEEE 802.15.4 networks using the OQPSK-DSSK (Offset Quadrature Phase-Shift Keying - Direct Sequence Spread Spectrum) modulation. The results show that using an algorithm named Flashflood, 94.88% end-to-end reliability can be achieved in a time-synchronized mesh network with 4 hops deployed in an environment with a high level of radio-frequency interference in the 2.4 GHz band.

Also at the physical layer, the authors of [13] evaluated the robustness of the BPSK (Binary Phase Shift Keying), OQPSK (Offset Quadrature Phase-Shift Keying) and 16-QAM (Quadrature Amplitude Modulation) modulations with OFDM (Orthogonal Frequency Division Multiplexing), which were introduced in IEEE 802.15.4g [1] SUN (Smart Utility Network) in 2015. The results show that using these modulations with OFDM provides a link robustness that is at least 6 dB better than DSSS-OPQSK, which was introduced in the original IEEE 802.15.4 [2] standard.

At the data-link layer, the authors of [14] experimentally demonstrate that channel hopping can be used to mitigate the effects of multi-path fading in low-power wireless networks based on the IEEE 802.15.4 standard. Based on these results, the authors of [15] evaluated to which extent can channel hopping mitigate the effects of multi-path propagation and internal/external interference and improve link reliability. The results show that channel hopping can reduce the number of re-transmissions by 56% compared to a single-channel approach.

Also at the data-link layer, the authors of [11] introduced and validated the concept of modulation diversity, which exploits the robustness properties of different modulations to increase link reliability. In [7] the authors evaluated an adaptive modulation selection strategy for packet re-transmissions, showing that with up to 2 re-transmissions per packet link reliability can increase from 93.8%

to 94.6% when compared to always using the same modulation for packet re-transmissions.

Finally, regarding the network layer, the authors of [6] studied the use of packet replication at the network layer to improve the end-to-end reliability by exploiting the disjoint paths available in a time-synchronized mesh network. The results show that packet replication improves the network reliability by a factor of 18 \times , while reducing the end-to-end latency by 40%.

In summary, the results show that constructive interference and channel hopping mechanisms can help coping with multi-path propagation and external interference. However, both techniques require network-wide time synchronization, which increases system complexity and impacts battery duration. In contrast, the results show that modulation diversity allows to improve link robustness, but it still cannot meet the target PDR requirements of industrial applications (i.e., PDR>99%). Finally, packet replication at the network layer can meet the PDR requirements of industrial applications. However, packet replication also requires a mesh network with time-synchronized nodes, increasing the deployment complexity and cost. Taking all this into account, in this paper we propose re-transmission shaping as a mechanism to improve link reliability in star networks without time synchronization requirements. However, please take into account that re-transmission shaping can also be used in mesh networks, or in conjunction with the other link reliability mechanisms presented earlier.

3 OVERVIEW OF THE RE-TRANSMISSION SHAPING MECHANISM

As introduced earlier, re-transmissions are a common mechanism used at the data-link layer to guarantee the delivery of data packets between an end-device and a gateway using a wireless communication technology. Whenever the acknowledgment packet from the gateway is not received at the end-device due to physical layer effects (i.e., multi-path propagation or internal/external interference), the end-device will re-transmit the original data packet again to provide another opportunity for the packet to be successfully received at the gateway. However, since physical layer effects are not deterministic and packet re-transmission increases end-device energy consumption and network load, a maximum number of re-transmissions per data packet is typically set. But assigning a fixed number of re-transmissions per packet may not be optimal, as if channel conditions are too adverse, the originating end-device could need more than the fixed number of re-transmissions to deliver a data packet and, hence, this would be lost.

Taking that into account, the aim of the re-transmission shaping mechanism that we present in this section is to dynamically adapt the number of maximum re-transmissions per packet according to channel conditions in order to meet both the data delivery requirements of the application and the target battery lifetime of end-devices. That is, given the average number of re-transmissions per data packet, the re-transmission shaping mechanism keeps track of the number of re-transmissions that have not been used to transmit previous data packets (i.e., if packets have been received by the gateway at the first transmission attempt). These unused re-transmission attempts are accumulated and can be used in the future when channel conditions are bad and the average number

of re-transmissions per data packet is not sufficient to guarantee successful delivery.

Considering this high-level description, we now focus on presenting the system model that defines how re-transmission shaping operates. For that, we assume that we have a network with n end-devices, with a battery of capacity C (mAh) that transmit a data packet with length L (bytes) and period T (seconds), and one gateway that receives the packets transmitted by end-devices. Upon successfully receiving a data packet from any end-device the gateway transmits an acknowledgment packet (ACK) back to the originating end-device. If the originating end-device does not receive the acknowledgment packet, either because the original data packet is not successfully received or the acknowledgment packet is lost, then the originating end-device re-transmits the data packet.

Considering the values of C , L and T , the average number of re-transmissions per data packet is N_{AVERAGE} and we assume that it is set to a value that allows to meet the battery lifetime of the device. That is, if $N_{\text{AVERAGE}}=3$ the device is allowed to perform 3 re-transmissions per data packet while operating for 1 year¹. Then, when the source end-device succeeds in transmitting a data packet i with a number X_i of re-transmissions, being $0 \leq X_i < N_{\text{AVERAGE}}$, the number $U_i = N_{\text{AVERAGE}} - X_i$ of unused re-transmissions can be accumulated for the re-transmission of subsequent data packets.

Hence, as depicted in Figure 1, the model of the re-transmission shaping mechanism is based on 5 variables N_{AVERAGE} , N_{MAXIMUM} , N_{ALLOWED} , N_{USED} and $N_{\text{AVAILABLE}}$, as described next:

- N_{AVERAGE} is an input value that represents the average number of re-transmissions per data packet that are allowed while ensuring the lifetime of the end-device. It is not required to be an integer, it can be directly derived from the device power constraint.
- N_{MAXIMUM} is an input value that represents the number of extra re-transmissions per packet that are allowed in addition to N_{AVERAGE} .
- N_{ALLOWED} is an output value that represents the maximum number of re-transmissions that are allowed for the current data packet being transmitted.
- N_{USED} is an input value that represents the number of re-transmissions that have been required to successfully deliver the previous data packet to the gateway.
- $N_{\text{AVAILABLE}}$ is an internal state variable that accumulates the number of re-transmissions that have not been spent in previous data packet transmissions and, hence, can be used in the future. It is initialized to zero.

Regarding N_{MAXIMUM} , notice that its value is set to avoid a given packet transmission that experiences bad instantaneous channel conditions to deplete all the N_{ALLOWED} re-transmissions available. Hence, its value has to be set depending on the context of each deployment. For environments presenting short deep drops in the link reliability it can be set to a high value, allowing to strongly increase the number of re-transmissions for short periods of time.

¹Of course, the exact values will depend on C , L and T , as well as the voltage and the transmit/receive current consumption of the radio transceiver, and the battery capacity, among others, but this discussion is out of the scope of the paper.

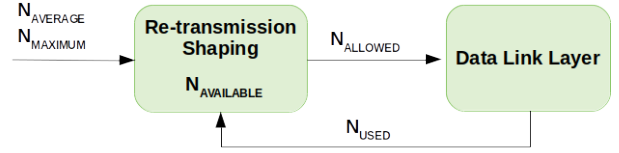


Figure 1: Diagram of the re-transmission shaping mechanism with the input (N_{AVERAGE} , N_{MAXIMUM} and N_{USED}), output (N_{ALLOWED}) and the internal state ($N_{\text{AVAILABLE}}$) variables, and its relationship with the data-link layer.

In contrast, for environments with long shallow drops in link reliability it can be set to a low value, allowing to extend the effects of re-transmission shaping for a longer period of time.

Using these variables, the operating principle of the re-transmission shaping mechanism is the following. Before a data packet transmission starts, the re-transmission shaping mechanism calculates the N_{ALLOWED} of re-transmissions available as

$$N_{\text{ALLOWED}}(k) = \text{floor}(N_{\text{AVERAGE}} + \min\{N_{\text{AVAILABLE}}(k), N_{\text{MAXIMUM}}\}). \quad (1)$$

so that, if unused re-transmissions are available, they are added to N_{AVERAGE} without exceeding the threshold set by N_{MAXIMUM} .

The N_{ALLOWED} value is then used by the physical layer to perform re-transmissions until the data packet is either successfully received (i.e., including the acknowledgment) or the number of re-transmissions becomes zero and no more re-transmissions can be performed. In either case, the re-transmission shaping module receives the number N_{USED} of re-transmissions used for that particular data packet and performs the following operation to update the internal $N_{\text{AVAILABLE}}$ variable:

$$N_{\text{AVAILABLE}}(k+1) = N_{\text{AVAILABLE}}(k) + (N_{\text{AVERAGE}} - N_{\text{USED}}(k)). \quad (2)$$

Notice that it cannot be negative because N_{USED} is always lower than N_{ALLOWED} , which depends on $N_{\text{AVAILABLE}}$ as in Equation 1.

Since in the first iteration $N_{\text{AVAILABLE}} = 0$, the formula that expresses $N_{\text{AVAILABLE}}$ for a generic time step k is

$$N_{\text{AVAILABLE}}(k) = \sum_{i=0}^{k-1} (N_{\text{AVERAGE}}(i) - N_{\text{USED}}(i)). \quad (3)$$

Notice that using these variables, the re-transmission shaping mechanism can emulate the usual re-transmissions strategy where N_{AVERAGE} is set to a constant value per data packet. This behavior can be achieved by setting N_{AVERAGE} to an integer value and making N_{MAXIMUM} equal to zero. In that case, for every data packet transmission the maximum number of re-transmission attempts is constantly equal to N_{AVERAGE} . In this case, the re-transmission shaping mechanism does not perform any additional task to the basic fixed number of re-transmissions case. In fact, as it can be noticed from Equation 1, despite $N_{\text{AVAILABLE}}$ increases, the value of N_{ALLOWED} is always upper bounded by N_{AVERAGE} . Hereinafter, we will refer to the particular case in which N_{MAXIMUM} is set to zero as *no re-transmission shaping* (i.e., noRS), as this represents the

base scenario that allows to compare the performance gains of our proposal.

4 EVALUATION METHODOLOGY

In this section, we present an overview of the data-set and a description of the simulator that we use to evaluate the re-transmission shaping mechanism presented in Section 3.

Throughout this section we use two performance metrics, the PDR (Packet Delivery Ratio) and the RNP (Required Number of Packets), that are widely used in low-power wireless communications [3]. On one hand, the PDR is defined as the ratio between the received and transmitted packets. On the other hand, the RNP is defined as the average number of re-transmissions required before a data packet is successfully received.

4.1 Data-set overview

To evaluate the re-transmission shaping mechanism we use a data-set of measurements obtained from a low-power wireless network deployed in an industrial warehouse to collect temperature, humidity, pressure and illumination measurements to monitor an HVAC (Heating, Ventilation and Air Conditioning) system. The network uses a star topology and consists of 11 OpenMote-B devices [10] that transmit periodic messages to a gateway using the IEEE 802.15.4g SUN modulations (i.e., SUN-FSK, SUN-OQPSK and SUN-OFDM). In addition to the physical measurements, the resulting data-set includes ~ 11 M entries with the RSSI (Received Signal Strength Indicator), CCA (Clear Channel Assessment) and packet delivery values for all 3 modulations of the IEEE 802.15.4g SUN standard, as shown in Table 1. More details regarding the deployment operation and the data obtained can be found in [12].

EUI-64 (last 2 bytes)	Received packets	RSSI (dBm)	CCA (dBm)	PDR (%)
56-53	924574	-84.0	-112.4	72.1
55-AD	1024664	-83.7	-115.5	79.9
55-E4	872200	-82.1	-111.2	68.0
55-99	897718	-96.2	-117.5	70.0
55-DD	1091950	-92.5	-117.3	85.1
55-65	1058746	-85.3	-118.3	82.5
56-0B	871477	-91.3	-118.4	67.9
56-32	1121696	-96.1	-119.9	87.4
55-B3	1076572	-95.0	-119.3	83.9
55-63	926221	-101.7	-118.1	72.2
63-0A	845050	-101.6	-119.0	65.9
Total/Mean	10710868	-91.8	-117.0	75.9

Table 1: Unique identifier (last 2 bytes of EUI-64), total received packets, and average RSSI (dBm), CCA (dBm) and PDR (%) values of the devices used in the deployment.

To simulate the data-link layer for the specific environment under analysis, a trace file for each end-device has been created from the original data-set. Each trace file contains PDR values for each IEEE 802.15.4g SUN modulation over time, which have been calculated by computing the frequency of successful transmissions over a window of n minutes ($n = 5$ was used in our analysis).

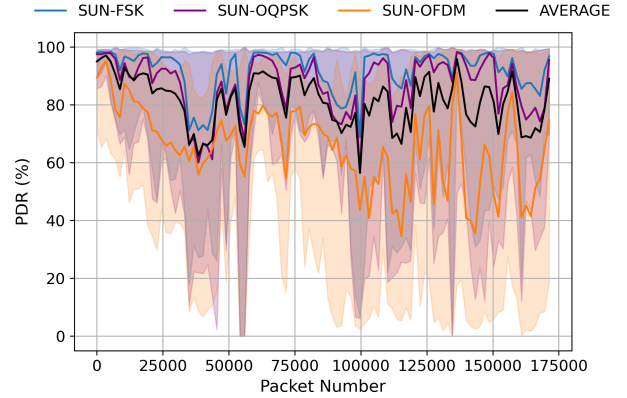


Figure 2: Median (solid line) and inter-quartile range (shaded area) of the PDR for the SUN-FSK (blue), SUN-OQPSK (purple) and SUN-OFDM (orange) modulations, and the median computed over all modulations’ PDR (solid black line). Median and inter-quartile range have been computed over PDR data stored in the trace file accumulated over one hour for all the devices in the data-set.

Notice that these windows do not overlap (i.e., each window starts where the previous one ends), and we have removed windows with PDR=0% if no successful transmission has been found within 75 minutes of the window center. Hence, for each minute in the original data-set time range, the trace file keeps a PDR value that is an estimate of the probability of a successful transmission for each IEEE 802.15.4g SUN modulation.

Figure 2 depicts calculated PDR values of the SUN-FSK, SUN-OQPSK and SUN-OFDM modulations for all devices present in the experiment. The solid lines represent the median, whereas the colored shadows represent the inter-quartile range computed over the accumulated PDR in one hour. On average, the PDR for the SUN-FSK, SUN-OQPSK and SUN-OFDM modulations is 81.3%, 80.7% and 65.7%, respectively. Notice that SUN-FSK and SUN-OQPSK provide substantially better PDR, but this can be explained by the fact that the radio transceiver used (i.e., Atmel AT86RF215) has a transmit power for the SUN-OFDM signal that is 6 dB lower. Regardless, it is important to notice that the instantaneous PDR values for individual devices and modulations can be 100% at given times or drop to values below 20% at other times. This is caused by the multi-path propagation and internal/external interference effects at the physical layer, and has a large impact on the target application.

4.2 Trace-based simulation

To evaluate the performance of the re-transmission shaping mechanism presented earlier we have developed a Python simulator² that implements the re-transmission shaping mechanism and uses the trace files presented earlier to simulate channel conditions.

To simulate the transmission of a given data packet the simulator first determines the value of $N_{ALLOWED}$ based on the values of $N_{AVERAGE}$, $N_{MAXIMUM}$ and $N_{AVAILABLE}$ of the re-transmissions

²The data-set and source code of the Python simulator are available in the following GitHub repository: https://github.com/wine-uoc/pewasun_2020.

shaping mechanism, as described in Section 3. Then, for each $N_{ALLOWED}$ the simulator determines which IEEE 802.15.4g SUN modulation to use using one of the two simple strategies available: *RANDOM* and *BEST*. In the *RANDOM* strategy the transmitting device randomly selects one of the three IEEE 802.15.4g SUN modulations available by sampling from a uniform distribution. In contrast, when using the *BEST* strategy the transmitting end-device always selects the modulation that has the best instantaneous PDR. Of course, the *BEST* strategy is an ideal scenario, as the instantaneous PDR value cannot be predicted in advance. However, using this strategy allows us to have an upper performance bound that allows to compare the performance of the *RANDOM* strategy to.

Once the modulation is selected, the channel simulator uses the PDR values for the given IEEE 802.15.4g SUN modulation and end-device, which have been obtained from the data-set, to determine if a the data packet transmission and its acknowledgment are successfully received or not. It does so by comparing a randomly generated number using a uniform distribution with the computed PDR value for the current data packet transmission. If the random value is below the computed PDR value the data packet is considered as successfully received. Otherwise, the data packet is considered as not successfully received. If the data packet is successfully received, the process is then repeated for the acknowledgment packet using the same PDR value and procedure. That is, the simulator assumes that links are symmetric and data packets are received according to a Bernoulli trial with probability equal to the computed PDR value.

The process is repeated until the data packet and the acknowledgment are successfully received or the number of transmissions for the current data packet reaches $N_{ALLOWED}$. If the data packet and the acknowledgment are successfully received, the channel simulator returns the number of transmissions used (N_{USED}) for the current packet to the re-transmission shaping module. On the contrary, if the data packet has not been successfully received the simulator returns 0 to the re-transmission shaping module, indicating that all transmission attempts have been used.

Finally, upon receiving N_{USED} value the re-transmission shaping mechanism updates the $N_{AVAILABLE}$ value according to Equation 2 and the process is repeated for the remaining data packet transmissions.

5 RESULTS AND DISCUSSION

This section presents and discusses the results obtained using the data-set and the channel simulator described in Section 4 using the values $N_{MAXIMUM} = 9$ and $N_{AVERAGE} = \{1, 2, 3, 6, 9\}$ presented in Section 3. We have selected these values experimentally, knowing that $N_{MAXIMUM} = 9$ re-transmissions per packet allows to reach a PDR > 99%, as required by our application, and setting $N_{AVERAGE} = \{1, 2, 3, 6, 9\}$ allows to explore the solution space that allows to reach the target PDR while minimizing the energy consumption.

5.1 Re-transmission shaping operation

As introduced in Section 3, the re-transmission shaping mechanism uses the average number of packets ($N_{AVERAGE}$), the maximum number of packets ($N_{MAXIMUM}$), the number of packets available ($N_{AVAILABLE}$), the number of packets allowed ($N_{ALLOWED}$) and the number of packets transmitted (N_{USED}) to operate.

Figure 3 shows the evolution of the number of packets allowed ($N_{ALLOWED}$) and the number of packets transmitted (N_{USED}) for every packet number in the simulation using the *RANDOM* strategy. The solid line represents the median and the shaded area represents the inter-quartile range of the two metrics, which have been computed using one hour-wide windows.

As it can be observed, for the device with low average transmit probability error values (i.e., EUI-16=55-AD depicted in Figure 3(a)) the variable $N_{ALLOWED}$ remains constant at $N_{MAXIMUM} = 9$, whereas the variable N_{USED} fluctuates between 1 and $9 + N_{AVERAGE}$ depending on the number of packet re-transmissions required for a given data packet. This indicates that the instantaneous transmit probability is good most of the times, allowing unused re-transmissions (i.e., $N_{ALLOWED} - N_{USED}$) to be accumulated for future use in $N_{AVAILABLE}$, as well as allowing the device to transmit more packets than defined by $N_{AVERAGE}$ to compensate for poor channel conditions.

In contrast, for the device with high average transmit probability error values (i.e., EUI-16=56-0B depicted in Figure 3(b)) the variable $N_{ALLOWED}$ drops to $N_{AVERAGE} = 3$ between packets 25000 and 45000, indicating that there are no additional re-transmissions to be used to compensate for the high average transmit probability error values. However, as channel conditions improve N_{USED} drops below 3 again, allowing $N_{AVAILABLE}$ to grow again and compensate for future channel impairments.

Last but not least, for the average of all devices (i.e., Figure 3(c)) notice how the N_{USED} average value is below 3 most of the times. This indicates that on average devices will be using less than 3 re-transmissions per data packet and, hence, the number of packets available in $N_{ALLOWED}$ will grow, allowing to compensate for future propagation or interference effects that cause high instantaneous transmit probability errors.

5.2 Evolution of performance metrics

As introduced in Section 4, we use the PDR and the RNP as the performance metrics to evaluate the re-transmissions shaping mechanism presented in Section 3.

Figure 4 presents the evolution of the PDR (a) and RNP (b) metrics for the *RANDOM* and *BEST* strategies with and without re-transmission shaping for $N_{AVERAGE} = 3$. The results are the average of all the devices present in the deployment.

As it can be observed, re-transmission shaping allows to increase the PDR for both the *RANDOM* and the *BEST* strategies. In particular, re-transmission shaping increases the PDR by 4.92% (from 0.935 to 0.981) for the *RANDOM* strategy and by 2.17% (from 0.969 to 0.990) for the *BEST* strategy. Regarding RNP, re-transmission shaping increases the average RNP for both the *RANDOM* and the *BEST* strategies. Specifically, re-transmission shaping increases the RNP by 40% (from 1.50 to 2.10) for the *RANDOM* strategy and by 27% (from 1.26 to 1.6) for the *BEST* strategy.

In turn, Figure 5 and Table 2 show the relation between the PDR and the RNP metrics for different values of average re-transmissions per packet (i.e., $N_{AVG} = \{2, 3, 6, 9\}$) and maximum re-transmissions per packet (i.e., $N_{MAXIMUM} = 9$). For $N_{AVERAGE} = 1$ we can observe that PDR is 77.4% and 88.9% for the *BEST* and *RANDOM* strategies regardless of whether re-transmission shaping is enabled or not.

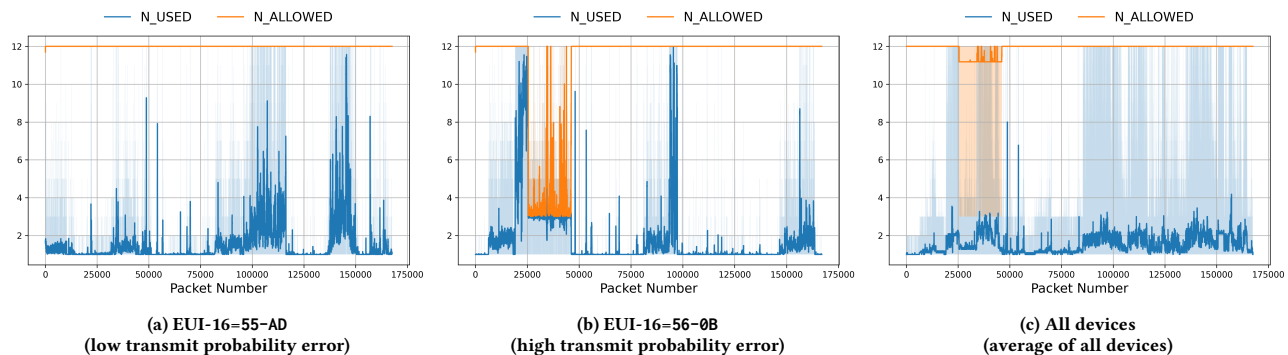


Figure 3: Temporal evolution of N_{USED} (blue) and $N_{AVAILABLE}$ (orange) values for two devices with low and high average transmit probability error (i.e., 55-AD and 56-0B, respectively) and the average values of these variables for all devices in the data-set. Notice that in all cases the devices use the *RANDOM* re-transmission strategy.

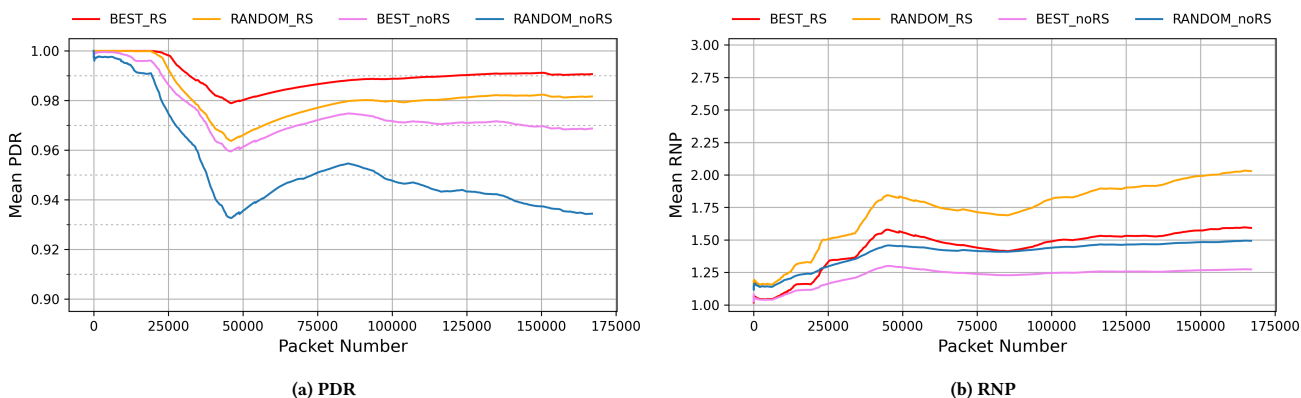


Figure 4: Temporal evolution of accumulated PDR (a) and RNP (b) values for the *RANDOM* and *BEST* strategies with and without re-transmission shaping using $N_{AVERAGE} = 3$ re-transmissions per data packet.

Also, for $N_{AVERAGE} = 1$ we have that $RNP = 1$ for all cases. Both results are expected, as we only allow one packet re-transmission per packet and, hence, the re-transmission shaping does not make any effect.

It is interesting to notice that for the *RANDOM* strategy with $N_{AVERAGE} = 2$ using re-transmission shaping the PDR improves by 6.9% (from 89.3% to 96.2%) while the RNP increases 35.9% (from 1.31 to 1.78). In contrast, adding another transmission attempt to the *RANDOM* strategy without re-transmission shaping would increase PDR by 4.6% (from 89.3% to 93.4%) while the RNP would increase by 13.7% (from 1.31 to 1.49). Of course, increasing the PDR is more difficult as its value approaches 100%, but the mean RNP value is still below the target (i.e., $N_{AVERAGE} = 2$). Adding more re-transmissions per packet allows to further increase the PDR at the expense of increasing the RNP and, hence, the energy consumption. With $N_{AVERAGE} = 6$ and re-transmission shaping the PDR reaches 98.8%, whereas with $N_{AVERAGE} = 9$ the PDR reaches 99.2%. Of course, the RNP raises to 2.20 and 2.35 respectively, indicating that more packets are required on average.

5.3 Discussion

In the previous subsections we have shown how the modulation shaping mechanism operates and how it can improve the PDR and RNP metrics compared to not using it.

As a summary of our findings, Figure 6 shows the percentage increment of the PDR (left) and RNP (right) performance metrics for the different $N_{AVERAGE}$ values (i.e., $N_{AVERAGE} = \{2, 3, 6, 9\}$) with respect to $N_{AVERAGE} = 1$ using the *RANDOM* strategy and with $N_{MAXIMUM} = 9$. As it can be observed, the benefits of using re-transmission shaping ranges from 24% to 28% in terms of PDR, whereas without re-transmission shaping the benefit of packet re-transmissions ranges from 15% to 26.5%. In contrast, in terms of RNP the energy overhead of using re-transmissions shaping ranges from 80% to 135%, whereas without re-transmission shaping the energy overhead is between 35% to 100%. Of course, the relative benefit of re-transmission shaping decreases as the PDR approaches 100%, whereas the RNP increases as more packets are required to sustain the PDR values.

Re-transmission		$N_{AVG} = 1$		$N_{AVG} = 2$		$N_{AVG} = 3$		$N_{AVG} = 6$		$N_{AVG} = 9$	
Shaping	Strategy	PDR	RNP	PDR	RNP	PDR	RNP	PDR	RNP	PDR	RNP
No	<i>RANDOM</i>	77.4%	1.00	89.3%	1.31	93.4%	1.49	97.1%	1.80	98.2%	1.98
	<i>BEST</i>	88.9%	1.00	94.8%	1.17	96.9%	1.27	98.6%	1.45	99.2%	1.56
Yes	<i>RANDOM</i>	77.4%	1.00	96.2%	1.78	98.2%	2.03	98.8%	2.20	99.2%	2.35
	<i>BEST</i>	88.9%	1.00	98.5%	1.51	99.1%	1.59	99.5%	1.72	99.6%	1.79

Table 2: Final PDR-RNP values for the *RANDOM* and *BEST* re-transmission strategies with and without the re-transmission shaping mechanism for $N_{AVERAGE} = \{2, 3, 6, 9\}$ and $N_{MAXIMUM} = 9$.

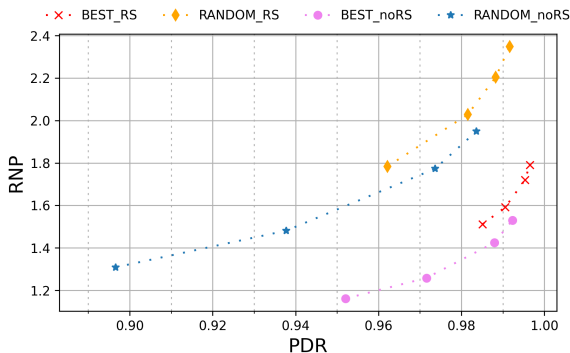


Figure 5: Final PDR-RNP values for the *RANDOM* and *BEST* re-transmission strategies with and without the re-transmission shaping mechanism. The results are presented for $N_{AVERAGE} = \{2, 3, 6, 9\}$ and $N_{MAXIMUM} = 9$.

If we compare the results presented using the *RANDOM* strategy for $N_{AVERAGE} = 1$ and $N_{AVERAGE} = 9$ without using the re-transmission shaping mechanism, we observe that the PDR increases by 26.9% (i.e., from 77.4% to 98.2%) and the RNP increases by 98% (i.e., from 1.00 to 1.98). Yet, the PDR does not reach the target value of our application (i.e., 98.2% instead of 99%) and the RNP is well below the $N_{AVERAGE}$ value (i.e., 1.98 instead of 9). In contrast, using the re-transmission shaping mechanism allows to further increase the PDR by 28% (i.e., from 77.4% to 99.2%) while increasing the RNP by 135% (i.e., from 1.00 to 2.35).

In summary, the proposed re-transmission shaping mechanism allows to increase the average PDR by better distributing data packet re-transmissions according to instantaneous channel conditions caused by multi-path propagation or internal/external interference. Of course, this may increase the average RNP compared to not using the re-transmission shaping mechanism, but the mechanism design ensures that the RNP is always kept below $N_{AVERAGE}$. Hence, an end-device with a battery designed to operate for 1 year with $N_{AVERAGE} = 9$ will increase its PDR while minimizing its RNP.

Based on these results, we can state that re-transmission shaping proves to be an interesting mechanism to increase the link reliability for low-power wireless networks, while allowing devices to operate for extended periods of time using batteries. In addition to that, we want to remark two aspects regarding the implementation of the re-transmission shaping mechanism. First, implementing

the re-transmission shaping mechanism is feasible in terms of the computational complexity and the memory capacity required considering the capabilities of the embedded micro-controllers that are typically used to implement low-power wireless networks. Second, implementing the re-transmission shaping mechanism is independent of the physical and data-link layers and, hence, it can be used to improve the reliability of wireless technologies other than IEEE 802.15.4g SUN.

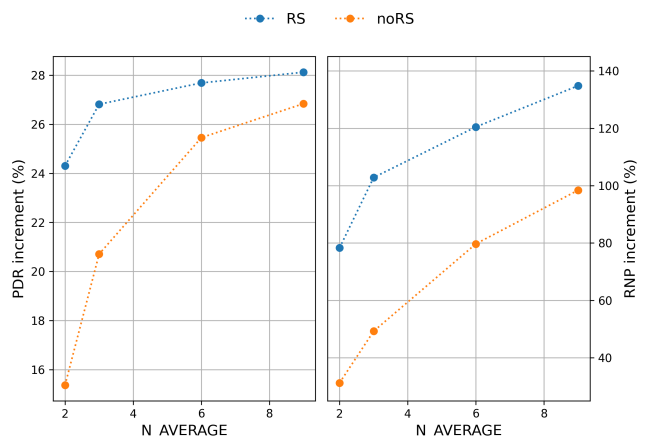


Figure 6: PDR (left) and RNP (right) percentage increment with respect to $N_{AVERAGE} = 1$ for the *RANDOM* strategy with $N_{MAXIMUM} = 9$. *RS* indicates using the re-transmission shaping mechanism, whereas *noRS* indicates not using the re-transmission shaping mechanism (as described in Section 3).

6 CONCLUSIONS

This paper has presented and evaluated the concept of re-transmission shaping as a means to increase the link reliability of low-power wireless communications. In summary, re-transmission shaping operates by keeping track of unused re-transmissions of data packets when wireless channel conditions are good, and allows additional re-transmissions of data packets when the channel conditions are bad, either due to multi-path propagation or internal/external interference effects. To evaluate the re-transmissions shaping mechanism we use trace-based simulations with the IEEE 802.15.4g SUN standard, and we use the PDR (Packet Delivery Ratio) and the RNP (Required Number of Packets) as the performance metrics

to assess its suitability. The results presented show that setting $N_{\text{AVERAGE}} = 9$ allows to reach a PDR of 99.2% with an RNP of 2.35. Compared to $N_{\text{AVERAGE}} = 1$, the PDR has increased by 27.34% (from 77.9% to 99.2%) and the RNP has increased by 235% (from 1.0 to 2.35). Yet, the average RNP does not reach 3 even for $N_{\text{AVERAGE}} = 9$, meaning that an end device designed to support $N_{\text{AVERAGE}} = 3$ for one year would still be able to operate after that period. Based on these results, we can conclude that re-transmission shaping is a useful tool to improve the link reliability of low-power wireless networks, as it can significantly improve PDR while sustaining a RNP below the target N_{AVERAGE} .

Given the potential of re-transmission shaping as a tool to increase link reliability for low-power wireless communications, in the future we will explore more advanced mechanisms to determine the number of re-transmissions that can be made available per data packet in order to further increase the PDR, while trying to maintain or reduce the RNP. In addition, we will also study the suitability of combining re-transmission shaping with other mechanisms targeted at improving link reliability of low-power wireless networks, such as adaptive modulation selection techniques, which have also demonstrated their potential in that regard.

ACKNOWLEDGMENTS

This research is partially supported by the Generalitat de Catalunya (SGR-60-2017) and the Spanish Ministry of Science, Innovation and Universities (SPOTS RTI2018-095438-A-I00) grants. This project is also co-financed by the European Union Regional Development Fund within the framework of the ERDF Operational Program of Catalonia 2014-2020 with a grant of 50% of total cost eligible (€4M).

REFERENCES

- [1] 2012. IEEE Standard for Local and Metropolitan Area Networks—Part 15.4: Low-Rate Wireless Personal Area Networks (LR-WPANs) Amendment 3: Physical Layer (PHY) Specifications for Low-Data-Rate, Wireless, Smart Metering Utility Networks. *IEEE Std 802.15.4g-2012 (Amendment to IEEE Std 802.15.4-2011)* (April 2012), 1–252.
- [2] 2016. IEEE Standard for Low-Rate Wireless Networks. *IEEE Std 802.15.4-2015 (Revision of IEEE Std 802.15.4-2011)* (April 2016), 1–709. <https://doi.org/10.1109/IEEESTD.2016.7460875>
- [3] Nouha Baccour, Anis Koubundefineda, Luca Mottola, Marco Antonio Zúñiga, Habib Youssef, Carlo Alberto Boano, and Mário Alves. 2012. Radio Link Quality Estimation in Wireless Sensor Networks: A Survey. *ACM Trans. Sen. Netw.* 8, 4, Article 34 (Sept. 2012), 33 pages. <https://doi.org/10.1145/2240116.2240123>
- [4] P. Bartolomeu, M. Alam, J. Ferreira, and J. A. Fonseca. 2018. Supporting Deterministic Wireless Communications in Industrial IoT. *IEEE Transactions on Industrial Informatics* 14, 9 (Sep. 2018), 4045–4054. <https://doi.org/10.1109/TII.2018.2825998>
- [5] T. Chang, T. Watteyne, X. Vilajosana, and P. H. Gomes. 2019. Constructive Interference in 802.15.4: A Tutorial. *IEEE Communications Surveys Tutorials* 21, 1 (2019), 217–237.
- [6] J. d. Armas, P. Tuset, T. Chang, F. Adelantado, T. Watteyne, and X. Vilajosana. 2016. Determinism through Path Diversity: Why Packet Replication Makes Sense. In *2016 International Conference on Intelligent Networking and Collaborative Systems (INCoS)*. 150–154. <https://doi.org/10.1109/INCoS.2016.105>
- [7] Ruan Gomes, Pere Tuset-Peiró, and Xavier Vilajosana. 2020. Improving Link Reliability of IEEE 802.15.4g SUN with Adaptive Modulation Diversity. In *2020 IEEE 31st International Symposium on Personal, Indoor and Mobile Radio Communications - (PIMRC)*. <https://doi.org/10.20944/preprints202003.0334.v1>
- [8] Remous-Aris Koutsiamanis, Georgios Papadopoulos, Tomas Lagos Jenschke, Pascal Thubert, and Nicolas Montavont. 2020. Meet the PAREO Functions: Towards Reliable and Available Wireless Networks. In *2020 IEEE International Conference on Communications (ICC)*.
- [9] Pascal Thubert, Dave Cavalcanti, Xavier Vilajosana, and Corinna Schmitt. 2020. *Reliable and Available Wireless Technologies*. Internet-Draft draft-thubert-raw-technologies-04. IETF Secretariat. <http://www.ietf.org/internet-drafts/draft-thubert-raw-technologies-04.txt> <http://www.ietf.org/internet-drafts/draft-thubert-raw-technologies-04.txt>
- [10] Pere Tuset-Peiró, Xavier Vilajosana, and Thomas Watteyne. 2016. OpenMote+: A Range-Agile Multi-Radio Mote. In *Proceedings of the 2016 International Conference on Embedded Wireless Systems and Networks (Graz, Austria) (EWSN '16)*. Junction Publishing, USA, 333–334.
- [11] Pere Tuset-Peiró, Ferran Adelantado, Xavier Vilajosana, and Ruan Gomes. 2020. Reliability through modulation diversity: can combining multiple IEEE 802.15.4-2015 SUN modulations improve PDR?. In *2020 IEEE Symposium on Computers and Communications (ISCC)*.
- [12] Pere Tuset-Peiró, Ruan D. Gomes, Pascal Thubert, Eva Cuerva, Eduard Egusquiza, and Xavier Vilajosana. 2020. A dataset to evaluate IEEE 802.15.4g SUN for Dependable Low-Power Wireless Communications in Industrial Scenarios. *MDPI Data* 5(3), 64 (2020). <https://doi.org/10.3390/data5030064>
- [13] Pere Tuset-Peiró, Francisco Vázquez-Gallego, Jonathan Muñoz, Thomas Watteyne, Jesus Alonso-Zarate, and Xavier Vilajosana. 2019. Experimental Interference Robustness Evaluation of IEEE 802.15.4-2015 OQPSK-DSSS and SUN-OFDM Physical Layers for Industrial Communications. *Electronics* 8, 9 (Sep 2019), 1045. <https://doi.org/10.3390/electronics8091045>
- [14] Thomas Watteyne, Steven Lanzisera, Ankur Mehta, and K. S. J. Pister. 2010. Mitigating Multipath Fading through Channel Hopping in Wireless Sensor Networks. In *2010 IEEE International Conference on Communications*. 1–5. <https://doi.org/10.1109/ICC.2010.5502548>
- [15] Thomas Watteyne, Ankur Mehta, and Kris Pister. 2009. Reliability through Frequency Diversity: Why Channel Hopping Makes Sense. In *Proceedings of the 6th ACM Symposium on Performance Evaluation of Wireless Ad Hoc, Sensor, and Ubiquitous Networks (Tenerife, Canary Islands, Spain) (PE-WASUN '09)*. Association for Computing Machinery, New York, NY, USA, 116–123. <https://doi.org/10.1145/1641876.1641898>